other planets, we gain critical insights into the habitability of exoplanets and the potential for magnetic fields to shield atmospheres from stellar radiation.]

The President. Thank you very much, Gabby. Questions? I have one. People often say that the last signal you can detect from Earth as you went away would be the auroral kilometric radiation (AKR). I am wondering if people are making predictions from the point of exoplanetary science on the difference between AKR, SKR, and JKR in terms of detecting what sort of planet we are talking about?

*Dr. Provan.* I do know that people are using radio signals to look for aurorae for different planets and extrasolar sources.

The President. These differences in the field-line-current systems for those sources are so fundamental that I think we should use that.

Dr. Stanley. We would have had some fantastic storms like the Carrington event that the ancient cave dwellers, in France, for instance, would have seen.

*Dr. Provan.* That is interesting when you look at the Northern Lights in myths and stories. That must also have occurred to the Romans and the Greeks given their latitude.

*Dr. Stanley.* Regarding the Carrington event, if you read his actual diary, rather than *Monthly Notices*, he did not continue his observations because he got back to cutting his trees. If you see the actual diary entry you will see that his arboreal interest supercedes his interest in astronomy.

A Fellow. I was looking to the future instead of the cave paintings. The JUICE mission is on its way to Jupiter and Ganymede now and I wondered what thoughts you might have both about what JUICE might discover about Ganymede and also Jupiter's aurora?

*Dr. Provan.* I had wanted to talk about Ganymede's aurora in this talk because it is the lack of wobbling of Ganymede's aurora that demonstrated that Ganymede has a salty, subsurface ocean. I'm looking forward to JUICE.

The President. Can I ask for a last round of applause for our James Dungey Lecturer. [Applause.] Thank you to Gabby and our other speakers tonight.

# REDISCUSSION OF ECLIPSING BINARIES. PAPER 26: THE F-TYPE LONG-PERIOD SYSTEM HP DRACONIS

By John Southworth

Astrophysics Group, Keele University

HP Dra is a well-detached eclipsing binary containing two late-F stars on an orbit with a relatively long period of 10·76 d and a small eccentricity of 0·036. It has been observed in 14 sectors using the *Transiting Exoplanet Survey Satellite (TESS)*.

We use these data plus literature spectroscopic measurements to establish the properties of the component stars to high precision, finding masses of  $1.135\pm0.002~M_{\odot}$  and  $1.098\pm0.002~M_{\odot}$  and radii of  $1.247\pm0.005~R_{\odot}$  and  $1.150\pm0.005~R_{\odot}$ . We find a much smaller third light than previous analyses, resulting in significant changes to the measured radii. These properties match theoretical predictions for an age of 3.5 Gyr and a solar metallicity. We present a spectrum of the Ca H and K lines in which chromospheric activity is visible from both components. The distance we find to the system,  $77.9\pm1.2$  pc, matches the Gaia DR3 parallax value of  $79.2\pm0.3$  pc.

### Introduction

This work continues our series¹ of reanalyses of known detached eclipsing binary systems (dEBs) using new photometric observations primarily from the NASA *Transiting Exoplanet Survey Satellite*² (*TESS*). The aim is to use space-based data³ to improve the measurements of the properties of the component stars and to add them to the *Detached Eclipsing Binary Catalogue*⁴ (*DEBCat*\*).

In this work we present a study of HP Draconis (Table I), a late-F-type system with an eccentric orbit of relatively long period. Its variability was first noticed in photometry from the *Hipparcos* satellite<sup>5</sup>, with a period of 6·693 d, and it was given its variable-star designation by Kazarovets *et al.*<sup>6</sup>. Its correct orbital period of 10·762 d was established by Kurpińska-Winiarska *et al.*<sup>7</sup> and refined by Milone *et al.*<sup>8</sup>.

Table I

Basic information on HP Draconis. The BV magnitudes are each the mean of 94 individual measurements<sup>12</sup> distributed approximately randomly in orbital phase. The JHK magnitudes are from 2MASS<sup>13</sup> and were obtained at an orbital phase of 0.89.

Property	Value	Reference
Right ascension (J2000)	18h54m53s·481	14
Declination (J2000)	+51°18′29″·79	14
Henry Draper designation	HD 175900	15
Hipparcos designation	HIP 92835	5
Tycho designation	TYC 3552-394-1	12
Gaia DR <sub>3</sub> designation	2144465183642116864	16
Gaia DR3 parallax (mas)	12·6153 ± 0·0516	16
TESS Input Catalog designation	TIC 48356677	17
B magnitude	8.54 ± 0.02	12
V magnitude	7·93 <b>±</b> 0·01	12
J magnitude	6·853 ± 0·020	13
H magnitude	6.616 <b>±</b> 0.016	13
$K_{\circ}$ magnitude	6·565 <b>±</b> 0·017	13
Spectral type	F9 V + F9 V	8

<sup>\*</sup>https://www.astro.keele.ac.uk/jkt/debcat/

Milone et al. presented an analysis of HP Dra, using radial velocities (RVs) from the Ca infrared triplet and the *Hipparcos* light-curve to simulate the then-expected performance of the *Gaia* mission. This work was updated by Milone, Kurpińska-Winiarska & Oblak (hereafter MKO10) using additional RVs and BV photometry from Cracow That analysis resulted in measurements of the stellar masses and radii to 1% precision. The previous finding of apsidal motion became only marginally significant in that analysis.

MKO10 found that 10% of the light in the system was produced by a source other than the two eclipsing stars, and noted that this was more than could be provided by nearby resolved stars contaminating the photoelectric photometry. They also presented cross-correlation functions in which no trace of a putative third component was visible. Possible explanations are that the additional light comes from an object with few spectral lines (e.g., a white dwarf) or from two or more stars none of which are individually identifiable in the spectra.

Jalowiczor *et al.*<sup>10</sup> identified the object *Gaia* DR2 2144465183642117888 as a white-dwarf companion to HP Dra, with a common proper motion and an angular distance of 14".405. As it is fainter by approximately 10 mag, it contributes a negligible amount of light to the *TESS* light-curve and thus is not responsible for the third light found by MKO10.

Baroch *et al.*<sup>11</sup> included HP Dra in their sample of dEBs expected to show apsidal motion dominated by the general-relativistic contribution. They analysed the first three sectors of *TESS* data but found no clear evidence for apsidal motion.

### Photometric observations

HP Dra has been observed by *TESS* in 14 sectors (14, 15, 26, 40, 41, 53, 54, 55, 59, 74, 75, 80, 82, 86). In all cases data are available at 120-s cadence, and these were used for our analysis below. Lower-cadence observations (200, 600, and/or 1800 s) are also available for all sectors but were not used due to their poorer time resolution. The data were downloaded from the NASA Mikulski Archive for Space Telescopes (MAST\*) using the LIGHTKURVE package<sup>18</sup>.

We used the simple aperture photometry (SAP) light-curves from the SPOC data-reduction pipeline<sup>19</sup> for our analysis, and removed low-quality data using the LIGHTKURVE quality flag "hard". The data were converted into differential magnitudes and the median magnitude was subtracted from each sector for convenience.

Fig. 1 shows the light-curve from sector 86; the remaining sectors are similar so are not plotted. Some variability is visible in sector 86 and others (*e.g.* at times around BJD 2460637·5 and 2460651·0). This variability recurs on the orbital period of *TESS* so is an instrumental signal, not astrophysical.

## Light-curve analysis

The components of HP Dra are well-separated and the light-curve is suitable for analysis using the JKTEBOP<sup>†</sup> code<sup>20,21</sup>. The profusion of data, the possibility of apsidal motion, and the expected change of third light with *TESS* sector, meant it was most efficient to model the light-curve from each sector individually.

<sup>\*</sup>https://mast.stsci.edu/portal/Mashup/Clients/Mast/Portal.html

<sup>†</sup>http://www.astro.keele.ac.uk/jkt/codes/jktebop.html

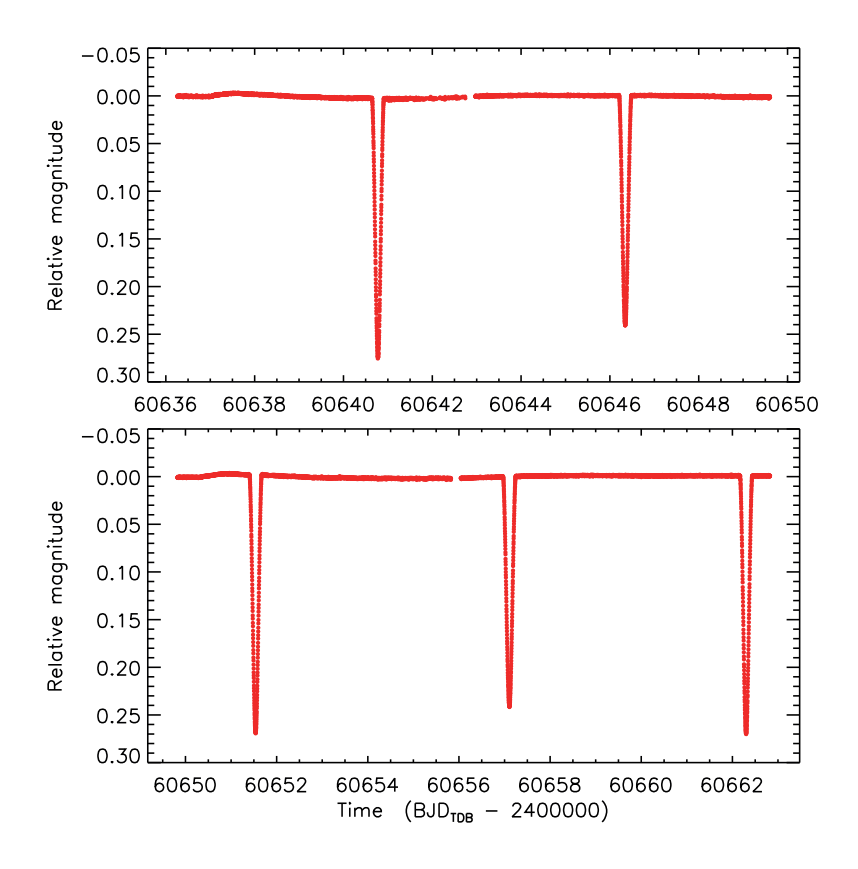


Fig. 1

TESS sector-86 photometry of HP Dra. The flux measurements have been converted to magnitude units after which the median was subtracted. The other 13 sectors used in this work are very similar so are not plotted.

The system is in eclipse for only approximately 10% of the time, so we removed data away from an eclipse to save computational time. This was done by detecting each fully-observed eclipse and retaining all data during eclipse plus an additional 0·1 d both before and after. Each eclipse was then normalized to zero differential magnitude by fitting and subtracting a straight line to the out-of-eclipse data, in order to remove slow variations of either instrumental or astrophysical origin.

For our analysis we defined star A to be the star eclipsed at the primary (deeper) minimum, and star B to be the one eclipsed at secondary minimum. The fitted parameters for each sector were fractional radii of the stars  $(r_A)$  and  $(r_B)$ , the central-surface-brightness ratio (f), third light  $(L_3)$ , orbital inclination (f) and eccentricity (f), argument of periastron (f), orbital period (f), and a reference time of primary minimum (f). The fractional radii were expressed as their sum (f) and ratio (f) and the shape parameters as the combinations f) or f) and f) and f) and f) and f) and f) and the shape parameters as the combinations f) or f) and the shape parameters as the combinations f) and f) and f) and f) are the primary minimum f).

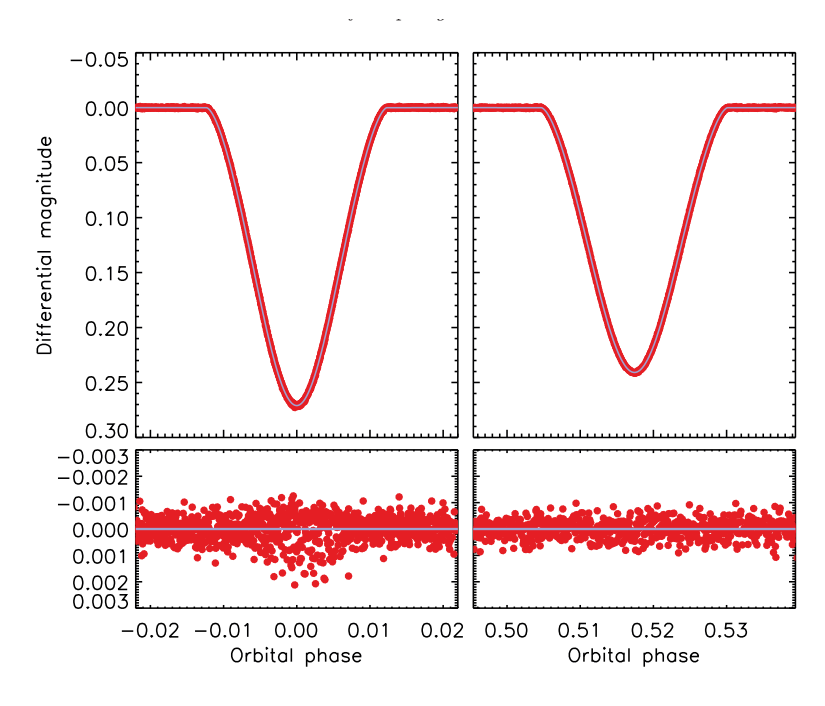


FIG. 2

JKTEBOP best fit to the light-curves of HP Dra from *TESS* sector 86 for the primary eclipse (left panels) and secondary eclipse (right panels). The data are shown as filled red circles and the best fit as a light-blue solid line. The residuals are shown on an enlarged scale in the lower panels.

TABLE II

Photometric parameters of HP Dra measured using JKTEBOP from the TESS light-curves.

The error bars are 10 standard errors and were obtained from the scatter of the results for individual sectors.

Parameter	Value	
Fitted parameters:		
Orbital inclination (°)	87·5554 ± 0·0060	
Sum of the fractional radii	0·08940 ± 0·00006	
Ratio of the radii	0·9220 ± 0·0071	
Central-surface-brightness ratio	o·95684 <b>±</b> o·00084	
Third light	0·0049 <b>±</b> 0·0020	
e cos ω	0.027355 ± 0.000005	
$e \sin \omega$	0·02411 <b>±</b> 0·00016	
LD coefficient c	0·6204 ± 0·0065	
LD coefficient $\alpha$	0.5548 (fixed)	
Derived parameters:		
Fractional radius of star A	0.04652 ± 0.00017	
Fractional radius of star B	0.04288 ± 0.00018	
Light ratio $\ell_{\rm R}/\ell_{\rm A}$	0·814 <b>±</b> 0·013	
Orbital eccentricity	0·03647 <b>±</b> 0·00011	
Argument of periastron (°)	41·31 ± 0·19	

parameters. Limb darkening (LD) was accounted for using the power-2 law<sup>22-24</sup> and we required both stars to have the same LD coefficients. The linear coefficient (c) was fitted and the non-linear coefficient ( $\alpha$ ) fixed at a theoretical value<sup>25,26</sup>. The *TESS* flux measurement errors were scaled to force a reduced  $\chi^2$  of  $\chi^2_{ij} = 1 \cdot 0$ .

We found good fits for all sectors, and that for sector 86 can be seen in Fig. 2. The results between sectors are also in good agreement. The unweighted mean and standard error of the values for each parameter can be found in Table II. Uncertainties were also calculated using Monte Carlo and residual-permutation algorithms, with similar results to the standard errors in Table II.

Our results for some parameters  $(i, e, \omega)$  are in good agreement with those that can easily be compared to the values from MKO10 (their table 4). We find a much smaller third light of 0.5% compared to their ~10%, and this changes the measured radii significantly.

## Orbital ephemeris

Our analysis above yielded a mean time of primary eclipse for each sector, which are useful for establishing a precise ephemeris. We fitted a linear ephemeris to the times, obtaining

$$Min I = BJD_{TDR} 2459790.615043(6) + 10.76154354(16)E$$
 (1)

where E is the number of cycles since the reference time of minimum and the bracketed quantities indicate the uncertainty in the final digit of the previous number. The root-mean-square of the residuals is 5·2 s and the  $\chi^2_{\nu}$  is 2·0. This relatively poor agreement may be caused by spot activity on the stars affecting the eclipse shapes (see below). The uncertainties in the ephemeris in Eq. 1 have been multiplied by  $\chi^2_{\nu}$  to account for this. The times of minimum are given in Table III and the ephemeris is plotted in Fig. 3. The relatively larger uncertainty in the timing from sector 59 is because there was only one fully-observed primary eclipse in these data.

Table III

Times of published mid-eclipse for HP Dra and their residuals versus the fitted ephemeris.

Orbital	Eclipse time	Uncertainty	Residual	TESS
cycle	$(B\mathcal{J}D_{TDB})$	(d)	(d)	sector
-102	2458692.937603	0.000036	0.000001	14
-99	2458725-222208	0.000022	-0.000024	15
-72	2459015.783904	0.000028	-0.000004	26
-36	2459403.199411	0.000024	-0.000064	40
-33	2459435.484155	0.000017	0.000049	41
-3	2459758-330385	0.000016	-0.000027	53
0	2459790.615020	0.000021	-0.000023	54
2	2459812-138137	0.000006	0.000007	55
12	2459919.753581	0.000047	0.000016	59
50	2460328.692216	0.000024	-0.000004	74
53	2460360-976867	0.000022	0.000016	75
65	2460490·115396	0.000021	0.000023	80
70	2460543.923052	0.000024	-0.000039	82
80	2460651-538493	0.000024	-0.000033	86

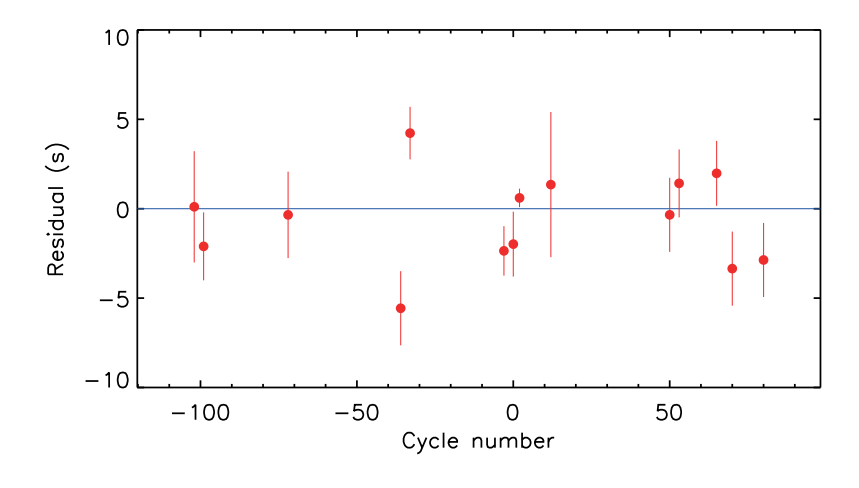


FIG. 3

Residuals of the times of minimum light from Table III (red circles) *versus* the best-fitting ephemeris. The blue solid line indicates a residual of zero.

We fitted a quadratic ephemeris as well, to see if apsidal motion was detectable, but the fit showed a negligible improvement and the quadratic variation was not significantly detected. We also tried to include historical times of minimum but found that they do not match the ephemeris above, suggesting the possibility of a light-time effect from a third body. We leave this matter to future work.

### Radial-velocity analysis

We have reanalysed the RVs presented by MKO10 for two reasons: to provide an independent analysis; and to obtain the velocity amplitudes ( $K_{\rm A}$  and  $K_{\rm B}$ ) needed for the next section (below). MKO10 performed a joint fit of their lightcurves and the RVs, and proceeded directly to the masses and radii without passing through the intermediate quantities  $K_{\rm A}$  and  $K_{\rm B}$ .

The RVs in MKO10 comprise three sets: 17 RVs per star from the *Coravel* cross-correlation spectrometer<sup>27</sup>, six spectra from the *Élodie* spectrograph<sup>28</sup> giving six RVs for star A and five for star B, and 29 spectra from the Asiago échelle spectrograph giving one RV per star per spectrum. The Asiago RVs were already published in Milone *et al.*<sup>8</sup>. We included all RVs in a single analysis, except for rejecting one discrepant Asiago RV taken near secondary eclipse.

We fitted all RVs simultaneously using JKTEBOP with a fixed P but allowing for a shift in  $T_0$ . We also fitted for  $K_{\rm A}$  and  $K_{\rm B}$ , the systemic velocity for both stars separately,  $e\cos\omega$ , and  $e\sin\omega$ . We also tried alternative approaches with  $e\cos\omega$  and  $e\sin\omega$  fixed at the photometric values and/or forcing the systemic velocities of the two stars to be the same, with essentially the same results but smaller error bars. The outcome of this analysis is the measurements  $K_{\rm A}=61\cdot971\pm0\cdot056~{\rm km~s^{-1}}, K_{\rm B}=64\cdot067\pm0\cdot060~{\rm km~s^{-1}},$  and the plot in Fig. 4. The RV fit yielded an insignificant phase shift versus our orbital ephemeris, and  $e\cos\omega$  and  $e\sin\omega$  consistent with the light-curve analysis. The error bars were obtained from 1000 Monte Carlo simulations  $^{29}$ .

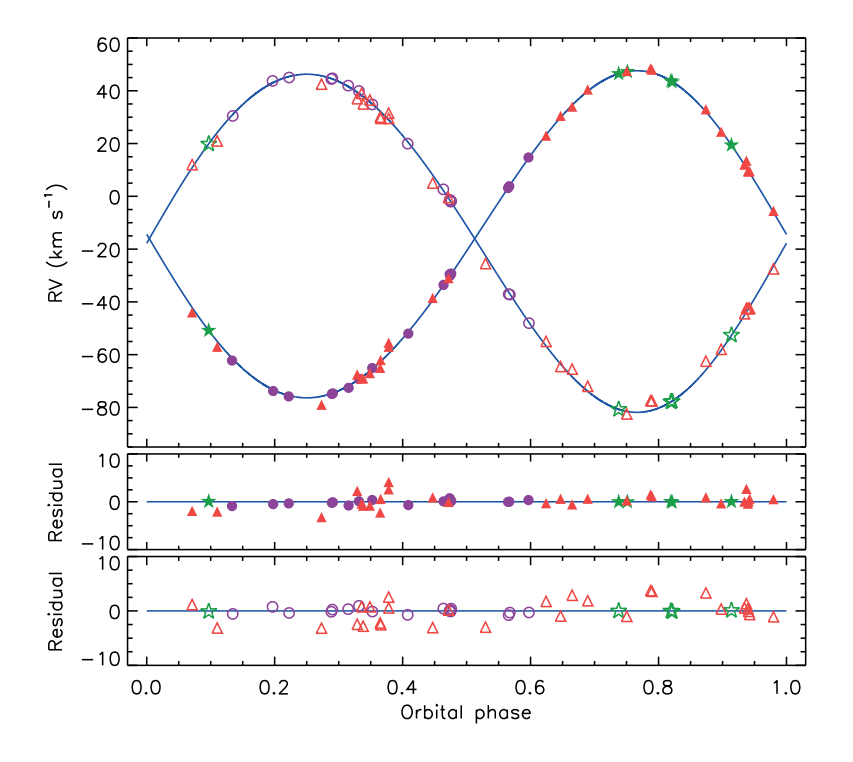


Fig. 4

RVs of HP Dra from MKO10 compared to the best fit from JKTEBOP (solid blue lines). The RVs for star A are shown with filled symbols, and for star B with open symbols. The residuals are given in the lower panels separately for the two components. RVs from *Coravel* are shown with purple circles, from *Élodie* with green stars, and from Asiago with red triangles.

### Physical properties and distance to HP Dra

We calculated the physical properties of HP Dra using the JKTABSDIM code with the photometric properties from Table II, and the  $K_{\rm A}$  and  $K_{\rm B}$  found above. We adopted the  $T_{\rm eff}$  of star A to be 6000±150 K from MKO10. For star B we calculated our own value based on that for star A and the surface-brightness ratio (Table II). The results are given in Table IV. Based on the data available, we have been able to measure the masses of the stars to 0.2% precision and the radii to 0.4% precision. These are among the most precise measurements currently available 32.4. Compared to MKO10 we find almost identical masses, as expected, but significantly different radii (1.247  $R_{\odot}$  and 1.150  $R_{\odot}$  versus 1.371  $R_{\odot}$  and 1.052  $R_{\odot}$ ). We attribute this discrepancy to the much greater quality and quantity of the TESS light-curves compared to previous ground-based datasets, and to our somewhat different photometric solution with much less third light.

### TABLE IV

Physical properties of HP Dra defined using the nominal solar units given by IAU 2015 Resolution B3 (ref. 30).

Parameter	StarA	Star B
Mass ratio $M_{\rm p}/M_{\rm A}$	0.9673	<u> </u> 0.0013
Semi-major axis of relative orbit $(R_{\circ}^{N})$	26.814 ±	Ł 0.012
Mass $(M_{\circ}^{\rm N})$	I·I354 ± 0·0023	I·0984 ± 0·0022
Radius $(R_{\circ}^{N})$	1·2474 ± 0·0046	1·1498 ± 0·0049
Surface gravity (log[cgs])	4·3012 ± 0·0032	4·3576 ± 0·0037
Density $(\rho_{\odot})$	o·5850 ± o·0064	0·7226 ± 0·0091
Synchronous rotational velocity (km s <sup>-1</sup> )	5·864 ± 0·021	5·406 ± 0·023
Effective temperature (K)	6000 ± 150	5935 ± 150
Luminosity $\log(L/L_{\circ}^{N})$	0·259 ± 0·044	0·170 ± 0·033
$M_{\rm bol}$ (mag)	4·09 ± 0·11	4·32 ± 0·11
Interstellar reddening $E(B-V)$ (mag)	0.00 7	- 0.0I
Distance (pc)	77·9 ±	I·2

We determined the distance to HP Dra using the BV magnitudes from  $Tycho^{12}$ ,  $JHK_s$  magnitudes from  $2MASS^{13}$ , and the surface-brightness calibrations from Kervella  $et~al.^{33}$ . No interstellar reddening was needed to align the optical and infrared distances, but we allowed an uncertainty of 0·01 mag for this deduction. Our most precise distance estimate is in the  $K_s$  band and is  $77.9 \pm 1.2$  pc; this is consistent with the distance of  $79.27 \pm 0.32$  pc from inversion of the Gaia DR3 parallax $^{14}$ .

We performed a comparison of the measured masses, radii, and  $T_{\rm eff}$  values of the component stars to theoretical predictions to infer their age and chemical composition. We found that a PARSEC I·2 theoretical model<sup>34</sup> with an approximately solar chemical composition and an age around 3·5 Gyr provides an adequate match to our results. We leave detailed analysis to the future, preferably once a spectroscopic metallicity estimate is available to provide another constraint on the theoretical models.

### Stellar activity

The TESS light-curve shows minor brightness modulations due to starspot activity, in addition to the instrumental variations discussed above. There are hints of a recurrence period of II·0 to II·5 d, in which case at least one of the stars is rotating slightly slower than the orbital period. The spot modulation evolves on a similar time-scale so this rotation period remains tentative. In a previous analysis of ZZ UMa<sup>37</sup> we found spot activity to be accompanied by a gradual change in the light ratio of the stars; this was searched for but not significantly detected in the current case.

In order to investigate the possibility of magnetic activity, we observed the Ca II H and K lines of HP Dra using the Intermediate Dispersion Spectrograph (IDS) at the Cassegrain focus of the Isaac Newton Telescope (INT). A single observation with an exposure time of 150 s was obtained on the night of 2022/06/07 in excellent weather conditions. We used the 235-mm camera, H2400B grating, EEV10 CCD, and a I-arcsec slit and obtained a resolution of approximately 0.05 nm. A central wavelength of 4050 Å yielded a spectrum

covering 373–438 nm at a reciprocal dispersion of 0-023 nm px<sup>-1</sup>. The data were reduced using a pipeline currently being written by the author<sup>38</sup>, which performs bias subtraction, division by a flat-field from a tungsten lamp, aperture extraction, and wavelength calibration using copper-argon and copper-neon arc-lamp spectra.

The spectrum was obtained at orbital phase 0.831 and is compared in Fig. 5 to a synthetic spectrum without chromospheric activity<sup>35,36</sup>. The Ca H and K line centres are clearly filled in by emission. The two stars had an RV separation of 118 km s<sup>-1</sup> at this time (0.156 nm at 396.85 nm) and double-peaked emission with this separation is apparent. We conclude that both stars show chromospheric emission due to spot activity, and spot modulation of at least one star is visible in the TESS light-curves.

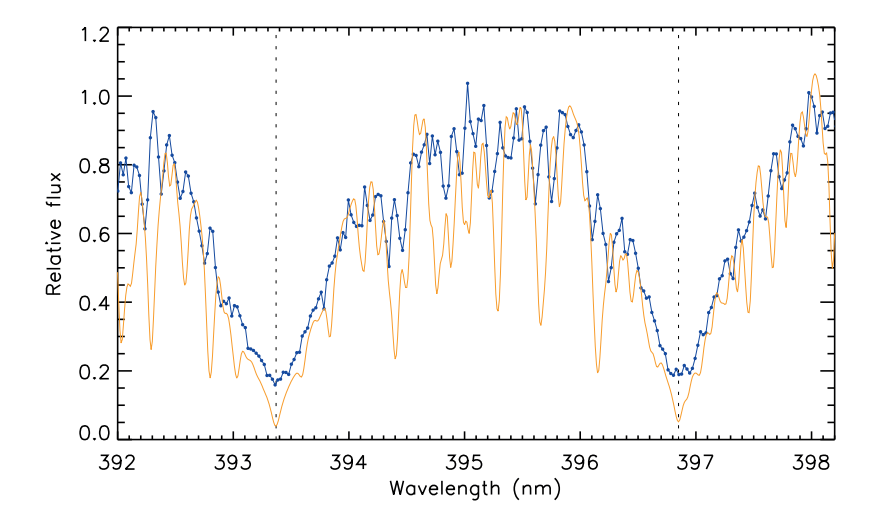


Fig. 5

Observed spectrum of HP Dra around the Ca II H and K lines (blue line with points) compared to a synthetic spectrum for a star with  $T_{\rm eff} = 6000$  K,  $\log g = 4.2$  and solar metallicity from the BT-Settl model atmospheres<sup>35,36</sup> (orange line). The H and K line central wavelengths are shown with dotted lines. The spectrum of HP Dra has been shifted to zero velocity and normalized to approximately unit flux.

### Summary and conclusions

HP Dra is a dEB containing two late-F stars in an eccentric orbit with a relatively long period of 10.76 d. It has a white-dwarf companion at an angular separation of 14''.4 and a hint of eclipse-timing variations caused by another, closer, companion. The *TESS* mission has observed it in 14 sectors, with full coverage of 63 eclipses (31 primary and 32 secondary). We modelled these lightcurves and published RVs to measure the physical properties of the system. These properties are matched by theoretical predictions for an age of 3.5 Gyr and an approximately solar metallicity. The distance we find agrees with that from *Gaia* DR3. Both stars exhibit chromospheric activity in the Ca H and K lines.

HP Dra would benefit from a detailed spectroscopic analysis to determine the photospheric chemical composition and improve measurements of the stellar  $T_{\rm eff}$  values. An analysis of its times of minimum light would also be helpful in checking for apsidal motion and the existence of a third body (in addition to the white dwarf). As the stellar masses are measured to 0.2% and the radii to 0.4%, and even without the suggested future work, the components of HP Dra are now among the most precisely characterized stars known.

## Acknowledgements

This paper includes data collected by the TESS mission and obtained from the MAST data archive at the Space Telescope Science Institute (STScI). Funding for the TESS mission is provided by the NASA's Science Mission Directorate. STScI is operated by the Association of Universities for Research in Astronomy, Inc., under NASA contract NAS 5-26555. This paper includes observations made with the Isaac Newton Telescope operated on the island of La Palma by the Isaac Newton Group of Telescopes in the Spanish Observatorio del Roque de los Muchachos of the Instituto de Astrofísica de Canarias. This work has made use of data from the European Space Agency (ESA) mission Gaia\*, processed by the Gaia Data Processing and Analysis Consortium (DPAC†). Funding for the DPAC has been provided by national institutions, in particular the institutions participating in the Gaia Multilateral Agreement. The following resources were used in the course of this work: the NASA Astrophysics Data System; the Simbad database operated at CDS, Strasbourg, France; and the arxiv scientific-paper-preprint service operated by Cornell University.

### References

- (I) J. Southworth, The Observatory, 140, 247, 2020.
- (2) G. R. Ricker et al., Journal of Astronomical Telescopes, Instruments, and Systems, 1, 014003, 2015.
- (3) J. Southworth, Universe, 7, 369, 2021.
- (4) J. Southworth, in Living Together: Planets, Host Stars and Binaries (S. M. Rucinski, G. Torres & M. Zejda, eds.), 2015, Astronomical Society of the Pacific Conference Series, vol. 496, p. 321.
- (5) The Hipparcos and Tycho Catalogues. ESA Special Publication, vol. 1200, 1997.
- (6) E. V. Kazarovets et al., IBVS, 4659, 1, 1999.
- (7) M. Kurpinska-Winiarska et al., IBVS, 4823, 1, 2000.
- (8) E. F. Milone et al., A&A, 441, 605, 2005.
- (9) E. F. Milone, M. Kurpinska-Winiarska & E. Oblak, A7, 140, 129, 2010.
- (10) P. A. Jalowiczor et al., RNAAS, 5, 170, 2021.
- (11) D. Baroch et al., A&A, 649, A64, 2021.
- (12) E. Høg et al., A&A, 355, L27, 2000.
- (13) R. M. Cutri et al., 2MASS All Sky Catalogue of Point Sources (The IRSA 2MASS All-Sky Point Source Catalogue, NASA/IPAC Infrared Science Archive, Caltech, US), 2003.
- (14) Gaia Collaboration, A&A, 674, A1, 2023.
- (15) A. J. Cannon & E. C. Pickering, Annals of Harvard College Observatory, 97, 1, 1922.
- (16) Gaia Collaboration, A&A, 649, A1, 2021.
- (17) K. G. Stassun et al., AJ, 158, 138, 2019.
  (18) Lightkurve Collaboration, 'Lightkurve: Kepler and TESS time series analysis in Python', Astrophysics Source Code Library, 2018.
- (19) J. M. Jenkins et al., in Proc. SPIE, 2016, Society of Photo-Optical Instrumentation Engineers (SPIE) Conference Series, vol. 9913, p. 99133E.
- (20) J. Southworth, P. F. L. Maxted & B. Smalley, MNRAS, 351, 1277, 2004.
- (21) J. Southworth, A&A, 557, A119, 2013.

<sup>\*</sup>https://www.cosmos.esa.int/gaia

<sup>†</sup>https://www.cosmos.esa.int/web/gaia/dpac/consortium

- (22) D. Hestroffer, A&A, 327, 199, 1997.
- (23) P. F. L. Maxted, A&A, 616, A39, 2018.
- (24) J. Southworth, The Observatory, 143, 71, 2023.
- (25) A. Claret & J. Southworth, A&A, 664, A128, 2022.
- (26) A. Claret & J. Southworth, A&A, 674, A63, 2023.
- (27) A. Baranne, M. Mayor & J. L. Poncet, Vistas in Astronomy, 23, 279, 1979.
- (28) A. Baranne et al., A&AS, 119, 373, 1996.
- (29) J. Southworth, The Observatory, 141, 234, 2021.
- (30) A. Prša et al., AJ, 152, 41, 2016.
- (31) J. Southworth, P. F. L. Maxted & B. Smalley, A&A, 429, 645, 2005.
- (32) P. F. L. Maxted et al., MNRAS, 498, 332, 2020.
- (33) P. Kervella et al., A&A, 426, 297, 2004.
- (34) A. Bressan et al., MNRAS, 427, 127, 2012.
- (35) F. Allard et al., ApJ, 556, 357, 2001.
- (36) F. Allard, D. Homeier & B. Freytag, Philosophical Transactions of the Royal Society of London Series A, 370, 2765, 2012.
- (37) J. Southworth, The Observatory, 142, 267, 2022.
- (38) J. Southworth et al., MNRAS, 497, 4416, 2020.
- (39) J. Southworth, The Observatory, 144, 181, 2024.

#### REVIEWS

Geniuses, Heroes and Saints. The Nobel Prize and the Public Image of Science, by Massimiano Bucchi, translated by Tania Aragona (MIT Press), 2025. Pp. 208, 23 × 15 cm. Price \$35 (about £,27) (paperback; ISBN 978 0

This is the second book I have reviewed about the Nobel Prizes. The first one 1 concentrated on a selection of Prizes awarded in topics related to astronomy and analysed the reasons for awarding the Prize in each case. This book is very different: it is a broad review of Nobel Prizes as a whole (i.e., all the Prizes awarded in the categories set out in Nobel's will), looking at the statistics and at how they affected the public view of science in general. It is an excellent translation (and slightly updated version) of an Italian original published in 2017.

The book starts with the origin of the Prize\* and closes with a list of all Nobel winners up to 2024 in the three scientific categories recognised in Nobel's will: Physics, Chemistry, and Physiology or Medicine (Literature and Peace are not significantly discussed in the book). In between, there are chapters with such intriguing titles as 'How do you win a Nobel Prize?', 'How Einstein won the Nobel Prize and why he almost never received it', and 'How not to win a Nobel Prize: the story of Lise [Meitner] and other Prize 'ghosts'' (people who deserved but didn't receive a Nobel Prize).

<sup>\*</sup>In 1888 April, Nobel (who developed dynamite) was shocked to read his own obituary in the paper, under the headline 'The Merchant of Death is Dead'. He realised that the journalist had confused him with his older brother Ludwig, who had died a few days earlier, but that the headline was aimed at him. Horrified that that would be how he would be remembered, he left a sum in his will to enable the foundation of a Prize for excellence in five fields — the three sciences listed above, literature and the promotion of peace — and indeed that is how he is remembered today.